Carbon Science

Vol. 8, No. 3 September 2007 pp. 214-224

Carbon Doping of TiO_2 for Visible Light Photo Catalysis - A review

K. Palanivelu[1,2], Ji Sun Im[1] and Young-Seak Lee[1,♠]

[1]Department of Nano Technology, Chungnam National University, Daejeon 305-764, Korea
[2]Center for Environmental Studies, Anna University, Chennai-600 025, India
♠e-mail: *youngslee@cnu.ac.kr*

(Received June 26, 2007; Accepted September 11, 2007)

Abstract

The field of photocatalysis is one of the fastest growing areas both in research and commercial fields. Titanium dioxide is the most investigated semi-conductor material for the photocatalysis applications. Research to achieve TiO_2 visible light activation has drawn enormous attentions because of its potential to use solar light. This paper reviews the attempts made to extend its visible photocatalytic activity by carbon doping. Various approaches adopted to incorporate carbon to TiO_2 are summarized highlighting the major developments in this active research field. Theoretical features on carbon doping are also presented. Future scenario in the rapidly developing and exciting area is outlined for practical applications with solar light.

Keywords : *Titania, Carbon doping, Solar light, Semi-conductor photocatalysis, Environmental applications*

1. Introduction

The pioneering work of Fujishima and Honda [1] in 1972 revealed that water splitting is possible by illuminating a titanium dioxide (TiO_2) electrode in an electrochemical cell. After their discovery much research has been undertaken in the last three decades to engineer a suitable photocatalyst material for water splitting in an electrochemical cell as well for degradation of organic contaminants. Among the various semiconductor materials, maximum attention has been given to TiO_2 because of its high photocatalytic activity, resistance to photocorrosion, photostability, low cost, and nontoxicity.

Titanium dioxide, also known as titanium(IV) oxide or titania, is the naturally occurring oxide of titanium with the chemical formula TiO_2. It appears in three crystalline polymorphic phases: rutile, anatase and brookite. The surface science of titanium dioxide has been thoroughly reviewed recently [2]. Among those, anatase TiO_2 exhibits the highest photocatalytic activity. The anatase, therefore, is the most effective and widely used photocatalyst. The principles and applications of photocatalysis have been excellently reviewed [3-8].

1.1. Mechanism of photocatalytic reactions

Valence electrons (electrons in the outermost orbit) are responsible for the bonding of atoms. When there are few atoms, the energy values of electrons in orbits are scattered. However, when the number of bonded atoms increases, the values become continuous within a certain range, rather than being scattered. This range is called as an "energy band". The area between two energy bands, where there is no electron energy, is referred to as a "forbidden band". Among the bands filled with electrons, the one with the highest energy level is referred to as the "valence band", (VB) and the band outside of this is referred to as the "conduction band" (CB). The energy width of the forbidden band between the VB and the CB is named as the "band gap". The band gap is like a wall that electrons must jump over in order to become free (Fig. 1). The amount of energy required to jump over the wall is referred to as the "band-gap energy". Only electrons that jump over the wall and enter the CB can move around freely.

Valence band electrons of titanium oxide need to move up to the CB when it is exposed to light of 380 nm or lower. At the same time, as many positive holes as the number of

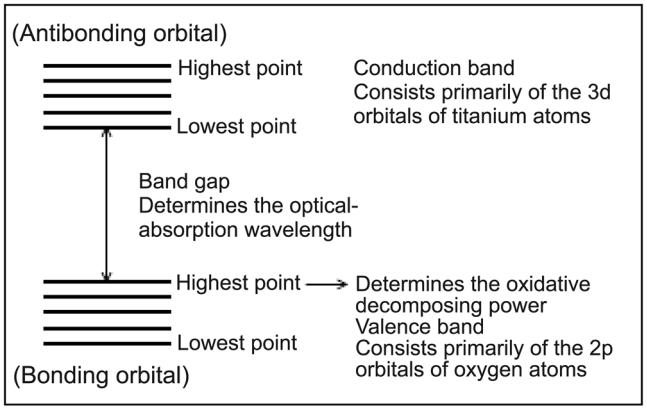

Fig. 1. Semiconductor band structure.

electrons that have jumped to the CB are created. Titanium oxide absorbs light having an energy level higher than that of the band gap, and causes electrons to jump to the CB to create positive holes in the VB. Despite the fact that the band gap value is 3.0 eV for the rutile type and 3.2 eV for the anatase type, they both absorb only ultraviolet rays. The anatase type exhibits higher photocatalytic activity than the rutile type. One of the reasons for this is the difference in the energy structure between the two types. In both types, the position of the VB is deep, and the resulting positive holes show sufficient oxidative power. However, the CB is positioned near the oxidation-reduction potential of the hydrogen, indicating that both types are relatively weak in terms of reducing power. It is known that the CB in the anatase type is closer to the negative position than in the rutile type; therefore, the reducing power of the anatase type is stronger than that of the rutile type. Due to the difference in the position of the CB, the anatase type exhibits higher overall photocatalytic activity than the rutile type. If energy is applied externally, electrons in the valence band can rise (this is referred to as "excitation") to the CB. Consequently, as many electron holes (holes left behind by the electrons moving up to the CB) as the number of excited electrons are created in the VB. This is equivalent to the movement of electrons from the bonding orbital to the antibonding orbital. In other words, the photoexcited state of a semiconductor is generally unstable and can easily break down. Titanium oxide, on the other hand, remains stable even when it is photoexcited. This is one of the reasons that titanium oxide makes an excellent photocatalyst. The schematic presentation of OH radical generation is shown in Fig. 2. The strong oxidative potential of the positive holes oxidizes water to create hydroxyl radicals (2.80 V) by TiO_2 for photochemical oxidation (PCO) of organic compounds. However, TiO_2 poor absorption in the visible region due its large band gap has restricted the utilization of solar energy to the UV portion, which is only ~4% of the solar energy. Thus, most of the solar spectrum goes to unutilized, because 45% of the energy

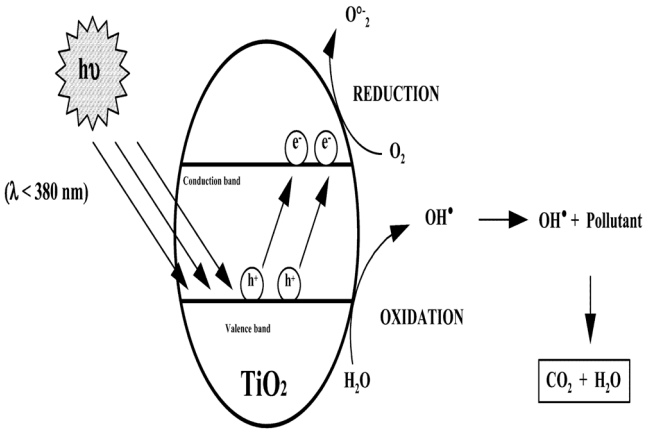

Fig. 2. Photocatalytic activity of TiO_2.

belongs to visible light.

1.2. Visible light activation of TiO_2

Consequently, various attempts have been made to improve the visible light activity. One strategy has been to coat the surface of TiO_2 surface with a thin layer of dye [9-12]. This method is known as dye sensitization and has been successfully applied to solar cell devices. However, the long term stability of the dye is the main question [13]. A great deal of effort has shown that doping with noble/transition metals, such as Pt, Au, Ag, Cr, Co, V, and Fe, extends the spectral response of TiO_2 well into the visible region and enhances the photoreactivity [14-22]. However, transition metal ion-doped TiO_2 suffers from some serious drawbacks, such as thermal instability and low quantum efficiency of the photo-induced charge carriers (electron-hole pairs). Further, low inter particle electron transfer rate, photocorrosion of the dopant, expensive and harmful nature of the doped materials are not favoring this approach. A good photocatalyst material must include the following properties.

(1) Band gap energy (approximately 2 eV band gap, with CB and VB edges)

(2) Position of the lowest point in the CB

(3) Position of the highest point in the VB

(4) Strong optical absorption in the visible and ultraviolet spectral regions

(5) Good stability in strong electrolytes and efficient charge transfer properties between the semiconductor and the electrolyte.

1.3. Carbon Modification of TiO_2

There are a significant number of experimental reports on the preparation of non-metal doped TiO_2 such as nitrogen [23-34], sulphur [35-39], fluorine [40-44] and carbon for extension of photocatalytic activity into the visible light region. Besides C-doped titania, TiO_2 with carbon composites have been prepared and used for PCO [45-53]. Carbon and TiO_2 combine to produce a composite material possessing the combined property of good adsorption and photocatalytic activity leading to an enhanced effect. Generally two possibilities of composites are possible; TiO_2 loaded on the AC [48] and carbon coating on the surface of titania [49]. In carbon coated TiO_2, a suitable organic compound is coated on the surface of TiO_2 followed by heating to yield a thin carbon layer covering TiO_2 particle. These types of materials had a carbon content of more than 2 wt% with a black color. Here the carbon not only act as a carrier, but also can be used as coating and pore agents. These biphasic composite materials have beneficial functions such as accumulating pollutants, capture intermediate products due to increase of effective surface area, prevent phase transformation of TiO_2 and grain growth. Though, these composite materials are

reported to be more effective than pristine TiO_2 in PCO, they are effective only with UV light. Further, it is expected that the efficiency of mineralization is usually lower due to the blocking of active sites by carbon. Surface modification with organic complexes also has been investigated for the photo-senstization of TiO_2 with UV light [54, 55]. However, a coordination metal complex via photoinduced sensitizer to TiO_2 is reported to be active with visible irradiation [56]. The long term stability of these complexes is to be established, since they are likely to be degraded similar to dyes. The main focus of this review, namely C-doped titania (CDT) with the view of using visible light in photocatalytic reaction is presented below.

2. Carbon doping of Titania

Addition of small amount of carbon impurity to TiO_2 in a controlled manner can be referred as C-doping of titania. The added C-impurity gives the semiconductor TiO_2 an excess of conducting electrons or an excess of conducting holes which is crucial for making visible light active. The carbon doped titania contained less than 1 wt% of carbon. The white color of the pure titania changed to grey/black depending on the amount of carbon in titania. The general chemical formula may be represented as TiO_{2-x} C_x and the x value varies depending on the preparation conditions (Refer Table 1). The incorporation of carbonaceous species may be responsible for the absorption tail in the visible-light region. The carbons in the doped samples may play the roles, such as

(i) it is the sensitizer for visible-light absorption,

(ii) it can also be the lattice defect of TiO_2 to form interface states that effectively lower the band gap.

2.1. Theoretical work on carbon-doping

In a semiconductor compound consisting of different atoms, the VB and CB formation processes are complicated, but the principles involved are the same. It is well known that the VB of titanium oxide is comprised of the 2p orbital of oxygen, while the CB is made up of the 3d orbital of titanium. In a semiconductor with a large band gap, electrons in the VB cannot jump up to the CB. However, modification of the band structure is essential to alter the light absorption characteristics of the TiO_2. With this in view, researchers have focused their attention to modify its band structure in such a way that the electron-hole pair is created on the VB and CB of the TiO_2 by absorbing the light from visible region. At the same time, the band edge position that is in the top of the VB and bottom of the conduction position should not be altered exceedingly. This may diminish the reduction and oxidation capability of the TiO_2 photocatalyst. Among the various methods to improve the visible light activation, the recent studies on doping of nonmetals like N, S, F, and C on TiO_2 lattice has opened a new door in the non-metal doping with significant expectation. Also, it is presumed that the mixing of empty and filled orbital of the doped hetero atoms with the energetically coordinated valence and conduction band orbital results in the broadening of the VB and CB. Theoretical results that demonstrate the doping of these non-metals on TiO_2 lattice results in broadening at the top of the VB, due to the contribution of 2p or 3p orbital of doped hetero-atom [23]. The position of heteroatom in the lattice plays a major role in the band structure and position. In the case of TiO_2, there are two different sites (interstitial and substitutional) possible for doping. The doping of hetero-atom in the substitutional position into the TiO_2 lattice alters the band more efficiently rather than the doping into the interstitial position. Also, the visible light photocatalytic activity depends on the concentration of the doped atoms.

Experimentally, it is known that oxygen vacancies exist in TiO_2 [57]. Despite experimental findings and improvements, the microscopic mechanism of visible-light absorbance in doped TiO_2 is still not well established. The structure and optical properties of carbon-doped titanium oxides, TiO_2, in the rutile and anatase forms have been investigated theoretically from density functional theory (DFT) first principles by Kamisaka. *et al.* [58]. They considered two possible doping sites namely carbon at an oxygen site anion doping and carbon at a titanium site cation doping and their calculated structures suggest [58], that cation-doped carbon atoms form a carbonate-type structure, whereas anion-doped carbon atoms (substitution on the oxygen site) do not invoke any significant structural change. Due to carbon substitution on the oxygen, a visible-light response was observed due to the appearance of an unoccupied impurity state occurring in the band gap. This optical response is beneficial in promoting photocatalytic degradation reactions, given the importance of electron holes in the VB in promoting this type of reaction. Further, they [58] have analyzed the Fermi level and suggested oxygen vacancies fill the in-gap impurity states by emitting electrons. Pair formation between doped carbon atoms and oxygen vacancies at a finite distance is expected to inhibit photocatalytic activity.

Valentine and co-workers [59] performed for both rutile and anatase TiO_2 carbon doping DFT calculations using generalized gradient approximation. At low carbon concentrations, they predicted that substitutional (to oxygen) carbon and oxygen vacancies are favored, whereas, under oxygen rich conditions, interstitial and substitutional (to Ti) C atoms are preferred. Higher dopant concentrations have been modeled by substituting three lattice O atoms of the 96-atom anatase super cell with three C atoms. This corresponds to an impurity concentration of 3%. The effect of carbon doping on the formation energy of oxygen vacancies can be illustrated by the following reactions.

$$TiO_2(s) - TiO_{2-x}(s) + xV_o + x/2\ O_2(g)\ (E_{f\_Vo} = 4.2\ eV) \quad (1)$$

$$TiO_2C_x(s) - TiO_{2-x}C_x(s) + xV_o + x\ 2O_2(g)(E_{f\_Vo} = 3.4\ eV) \quad (2)$$

$$TiO_{2-x}C_x(s) - TiO_{2-2x}C_x(s) + xV_o + x\ 2O_2(g)\ (E_{f\_Vo} = 1.9\ eV) \quad (3)$$

The first of these reactions represents the formation of an oxygen vacancy in undoped TiO_2. With the super cell, the corresponding energy (computed with respect to $1/2O_2$) is $E_{f\_Vo} = 4.2$ eV. In the presence of interstitial carbon (second reaction), the same process costs 3.4 eV: this is the sum of the energies needed to break both the C-O and Ti-O bonds. Even more remarkable, the presence of substitutional carbon (third reaction) reduces E_{f_Vo} to 1.9 eV, which is less than half the value computed for the nondefective bulk oxide. This effect was ascribed to the tendency of substitutional C atoms to accept excess electrons from the oxygen vacancy. Here substitutional carbon is a deep electron trap that competes with the Ti 3d states to accommodate extra charge generated by doping (e.g., via the addition of alkali metals) or by the formation of substoichiometric oxides.

The impurity states are attributable to both substitutional C atoms replacing O atoms, and to interstitial C atoms. These species are likely to be simultaneously and synergically present in anatase TiO_2. The results are different when carbon replaces titanium, because no states are found in the band gap, but only a small band gap shrinking. This could account

Table 1. Summary of carbon doped titania methods

Sl. No.	Precursor & Method of doping	Observations/Remarks	Application tested	Reference
1.	Ti-alkoxide, sol-gel hydrolysis process and calcination at 250°C	Formation of highly condensed carbonaceous species, DRS shift towards visible light, Long term stable semi-conductor evident from photocurrent study, Up to 0.6% carbon incorporation, Heating above 400°C no carbon in TiO_2 and no visible photocatalytic activity	p-Chlorophenol degradation with above 400 nm	Lettmann *et al.* 2001 [64]
2.	Controlled combustion of Ti metal in a natural gas flame at about 850°C	n-$TiO_{2-x}C_x$ where x is ~0.15, Absorbs up to 535 nm with a band gap energy of 2.32 eV, Photoconversion efficiency 8.4%	Water splitting	Khan *et al.* 2002 [65]
3.	Hydrolysis reaction with $TiCl_4$ and tetrabutyl ammonium hydroxide followed by calcinations at 550°C	Carbonate species formed confirmed by XPS and IR, DRS-absorption at 400-700 nm, Maximum band gap narrowing 0.14 eV, carbon incorporated in TiO_2 up to 2.98%, Presence of surface states close to the valence band edge	Oxidation of gaseous acetalaldehye, benzene and CO	Sakthivel and Kisch, 2003 [60]
4.	High temperature oxidation of TiC at 350-800°C in air	XPS broad peak around 289.0 eV due to carbonate compound, No evidence of visible light absorption	UV light decomposition of MB dye and water decomposition to form H2 gas	Choi *et al.* 2003 [66]
5.	High temperature oxidation of TiC at 350°C	XPS & XRD prove C-doped anatase, DRS of doped sample shifted to low energy region (red shift)	MB dye degradation in the range of 420-500 nm	Choi *et al.* 2004 [67]
6.	–	Absorption edge of carbonate species doped TiO_2 shifted from 400-700 nm	MB dye degradation with 550 nm light	Ohno *et al.* 2004 [68]
7.	TiC oxidative annealing at 800°C for 2 h	Rutile form with band gap of 2.95 eV	Acetaldehyde oxidation	Martyana *et al.* 2004 [69]
8.	Anodization of titanium foil followed by propane flame annealing for 3 min	Significant enhancement in the visible spectrum (400-700 nm), highest carbon content up to 5.6% in doped material, XPS peak of C-C(285.3 eV), CO(286.5 eV), and COO(289.0 eV). No Ti-C signal at 281.9 eV	Photo current generation	Shankar *et al.* 2005 [70]
9.	Hydrolysis reaction with $TiCl_4$ and tetrabutyl ammonium hydroxide followed by calcinations at 400°C in air	carbon-doped materials consisted of pure anatase modification (101 reflex, 12.64°; 200 reflex, 24.02°-XRD, Diffuse reflectance spectra reveal that the new absorption at 400-700 nm is related to the carbon content, Band gap energies of 3.02 and 3.11 eV were obtained for TiO_2-C1a and TiO_2-C1b, assuming that both are indirect semiconductors, like unmodified titania, total photocurrent as well as the surface photovoltage of the doped materials decreased markedly in relation to the undoped one, lack of reactivity with water.	Formic acid decomposition	Neumann *et al* 2005 [71]

Table 1. Continued

Sl. No.	Precursor & Method of doping	Observations/Remarks	Application tested	Reference
10	$TiCl_4$ and TBAH (pH 5.5), 600°C for 3 h	Brown colored product with 3.2% incorporation, band gap 2.85 eV, XPS core level at 281.82 eV(C 1s), doped sampled active electrochemical response	–	Reddy *et al.* 2005 [72]
11	Tetrabutyl orthotitanate by sol-gel method followed by calcinations at 150-600°C	Yellow to brown below 300°C calcinations and colorless above 300°C, High temp. above 500°C increase size of particle and lowers photo activity, Deactivation of the catalyst due to coverage of adsorbed NO_3^-.	NOx oxidation	Tseng *et al.* 2006 [73]
12	Sol gel process and calcinations at 150 & 200°C	Mixed phase of anatase, rutile, brookite and amorphous with carbonaceous species formation evident from Raman spectra, high photo activities in the visible range(above 400 nm) with bandgap of ~2.7-2.8 eV, carbon incorporation helps in phase transformation	–	Chou *et al.* 2006 [74]
13	TiC powder oxidation at 350°C for 8 h	36 nm red shift by C-TiO_2 with band gap of 29 eV, carbon incorporation is 0.7%, no improvement with iron doping its photoactivity	Tricholoro acetic acid degradation	Shen *et al.* 2006 [75]
14	Film deposition on glass plates by sputtering Ti metal under CO_2/Ar gas mixture in a RF magnetron sputtering apparatus	Ti-C bond peak at 282 eV (XPS), Narrowing band gap due to mixing of C 2p and O 2p, carbon content (0.7-1.1 mol%), UV irradiation of doped material resulted in more hydrophilicity doped carbons located at the oxygen sites, Shift in absorbance edge and shoulder to a longer wave length region	–	Irie *et al.* 2006 [76]
15	$TiCl_4$ & glucose solution spray pyrolysis followed by calcinations in air at 400-850°C for 5-10 min	XRD peaks at 36.1 and 61. 3 due to oxycarbide of TiOx Cy, Temp.above 700°C resulted in rutile structure, Bandgap narrowing from 3.20 to 2.82 & 2.63 eV for calcinations in air at 500°C and in Ar at 700°C, photocurrent stability test indicated good stability film.	Water splitting	Xu *et al.* 2006 [77]
16	Ti foil anodizing and annealing at 400C for 1 h followed by CO treatment at 500-800°C	Higher photocurrent density for $TiO_{2-x}C_x$ nano tube than TiO_2, band gap narrowing to 2.22 eV	Water splitting	Park *et al.* 2006 [78]
17	Thin film from titanium(IV) tetraisopropoxide with annealing at 450C for 6 h, carbon incorporation with hexane at 500°C for 4 h	Dark black colored material, small increase in optical density between 400-500 nm carbon content is low 0.1 At% with carbon on the surface of TiO_2, Re-oxidation for 30 min is needed for better incident photon-to-current conversion efficiencies (IPCE)	–	Enache *et al.* 2006 [79]
18	Ti sheet oxidation (flame pyrolysis) with methane	XRD spectra shows rutile structure, no evidence of Ti-C bond due to high temp., low temp. (700°C) gave best photocurrent results	Water splitting	Barnes *et al.* 2006 [80]
19	Anodization of Ti sheet followed by natural gas flame treatment at 820°C	Eight times more photo-response of D-doped TiO_2, carbon content is 1.8-3.7% with rutile form, band gap reduction to 2.84 eV, two fold increase in photocurrent density	–	Xu *et al.* 2007 [81]
20	Spray pyrolysis of glucose containing $TiCl_4$ solution	C-doping reduced the band gap energy to 2.78 eV and created a new energy band which lies above 1.45 eV above valence band, increase in C content enhanced the photoresponse of doped films	–	Xu & Khan, 2007 [82]
21	Hydrolysis of titanium isopropoxide & heating with glucose at 160°C for 12 h	Doping of C prohibit formation of brookite, doped catalysts absorbs more light in the range of 400-480 nm, incorporation of C can slightly improve the surface area, band gap lowering to 3.01 eV	RhB dye degradation	Ren *et al.* 2007 [83]
22.	Anodization of Ti foil followed by thermal acetylene treatment at 500°C	Surface doping than bulk doping observed, Good photo response over the whole range of visible light up to the near IR region (1.5 eV)	–	Hahn *et al.* 2007 [84]

for the slight reduction of the optical threshold energy in the ultraviolet (UV) region observed experimentally [60], but not for the enhanced absorption in the visible region. The concomitant presence of C species and O vacancies has been observed experimentally, with X-ray photoelectron spectroscopy (XPS) and electron paramagnetic resonance (EPR) and responsible for the improved photocatalytic activity in the visible region [61]. Carbon impurities result in modest variations of the band gap but induce several localized occupied states in the gap, which may account for the experimentally observed red shift of the absorption edge toward the visible. Carbon doping may favor the formation of oxygen vacancies in bulk TiO_2.

The electronic properties of N- and C-doped titania was analyzed by Lee *et al.* [62] using first principles density – functional calculations. They suggested that the red shift of optical absorption of doped material is related to the presence of isolated C 2p states in the band gap of TiO_2 rather than a band gap narrowing. Coupling of the top most C 2p state with Ti 4d state and this interaction between the C impurity and its neighboring Ti atoms in C-TiO_2 is relatively more than N-doped TiO_2. Xu [63] also reported a similar prediction based on band structural studies that the visible light activity is due to the isolated impurity states in the band gap.

2.2. Experimental studies on C-doping

2.2.1. Preparation methods

Various titanium and carbon precursors that have been used for the preparation of CDT are summarized in Table 1. It is clear from this table, the preparation methods used are hydrolysis followed by thermal treatment, Ti metal burning in flame, oxidative annealing of TiC, spray pyrolysis of Ti and C –precursors and Ti metal sputtering and then RF treatment with CO_2 also utilized. The Ti precursors employed are titanium alkoxides-tetrabutyltitanate (TBT) and titanium tetra-isopropoxide (TTP), Ti metal, $TiCl_4$, and TiC with carbon sources such as CO, CO_2, methane, natural gas, hexane, acetylene, alkoxides, carbide and tetrabutyl ammonium hydroxide (TBAH). Heat treatments up to 600°C yield anatase and above 800°C the rutile type. Presence of carbon is reported to prevent phase transformation [79]. However, crystal phase depends on the temperature and preparation conditions.

2.2.2. Spectral studies of doped material

Characterization of the prepared CDT catalyst was carried out by instrumental methods such as XRD, XPS, IR, Raman and UV-visible to confirm the doping and nature of materials. SEM/TEM also used to know the morphology [64-82]. All the researchers observed a color change and the color varies from yellow to black depending on the method of preparation [64, 72, 73, 79]. In the UV-visible diffuse

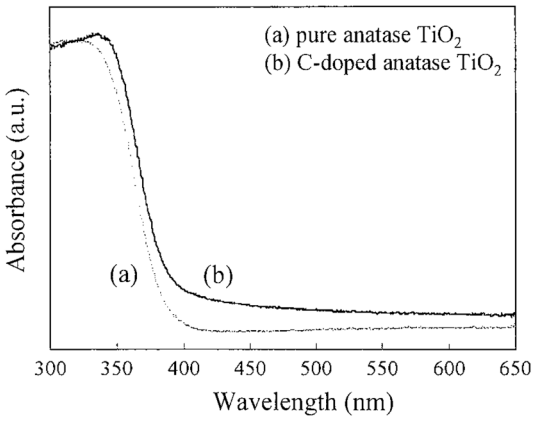

Fig. 3. UV-visible diffuse reflectance spectra of pure titania and C-doped. (Source Ref: 67)

reflectance spectra (DRS) of doped TiO_2 samples, a noticeable shift in the absorption edges was observed (Fig. 3). The new absorption in the range 400-600 nm is related to the carbon content. This noticeable shift of the optical absorption edges of the doped TiO_2 systems toward the visible regions of the solar spectrum. Notably, this shift towards the longer wavelengths originates from the band gap narrowing of titanium dioxide by carbon doping and the band gap energy (Eg) of the doped samples determined from the equation,

$$Eg = 1239.8/\lambda \quad (4)$$

where λ is the wavelength (nm) of the onset of the spectrum. This lead to band gap lowering and up to 2.3 eV has been reported [65, 78]. This implies that doping introduces electronic states in the band gap that are spread across the band gap, resulting in a diffused absorption spectrum. Because the doped samples have lower band gap energies than the undoped TiO_2 (3.00-3.2 eV), these doped photocatalysts are, therefore, likely to useful under visible light illumination.

The infrared (IR) spectrum of the C doped TiO_2 film shows several peaks between 2800 and 3000 cm^{-1} are assigned to organic compound remained in the materials. The peaks around 2350 cm^{-1} are the structure of CO_2. The peak at 1741 cm^{-1} was assigned to the –COOH of acetic acid in the sol. In the low frequency part of the spectra, many fluctuant bands develop around 500 cm^{-1} is attributed to the anatase phase of TiO_2. The peak at 1719 cm^{-1} was attributed to carbonate. IR spectrum of TiO_2-C which exhibits low-intensity peaks at 1738, 1096, and 798 cm^{-1} which are indicative for the carbonate ion [60, 88].

The Raman spectra of the points indicated in the spatial positions in the spectral mapping [74]. The Raman shifts around 400, 520, and 640 cm^{-1} were assigned to the anatase phase, two peaks on 325 and 360 cm^{-1} are for the brookite phase and around 440 and 610 cm^{-1} are for the rutile phase. Mixed anatase and rutile (or brookite) phases were observed

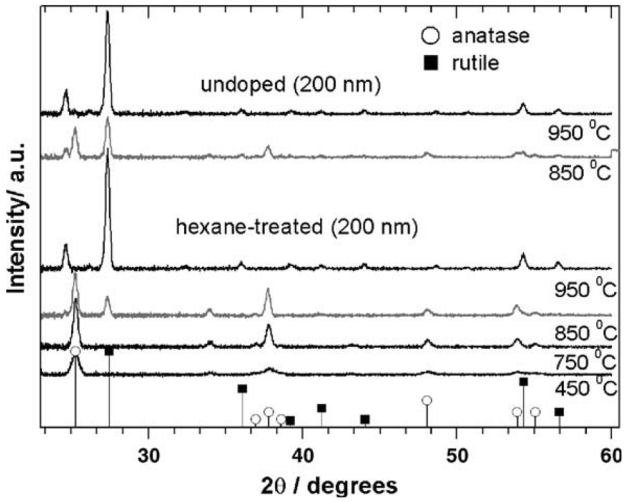

Fig. 4. XRD spectra of doped and undoped titania. (Source: Ref 79).

on doped samples. It is possible that the existence of rutile grains and the mixed surface structures effectively reduced the band gap by introducing some interface states in the prepared samples. The formation mechanism of the mixed phases is perhaps assisted by the impurities like carbonaceous species existing on the prepared TiO_2 surface followed by the calcination of the samples that transformed the amorphous phase to the more stable rutile phase in lower temperature. Detailed confocal Raman mapping showed that carbon structure also coexists with the rutile phase.

Fig. 4 shows the X-ray diffraction (XRD) spectra of undoped and hexane-treated TiO_2 after thermal treatments at increasingly higher temperatures [79]. At 850°C, the relative amount of rutile in hexane-treated TiO_2 is less than that for undoped TiO_2, which is indeed consistent with the assumption that a small amount of carbon is present in the bulk of the material. A similar series of measurements carried out by the authors on carbon-doped TiO_2 samples made by spraying under a CO_2 atmosphere. The transformation to rutile is much more strongly suppressed, and no traces of rutile are found even. The crystal nature is a function of calcining ambient, temperature, and carbon source concentration during doping. Below 500°C, the samples show the anatase structure. As the calcining temperature was increased to 700°C, the C-doped samples consist of significant rutile structure as well as the anatase, and its crystallinity greatly improved. It is important to note that they exhibit the presence of TiO_xC_y, identified by the peaks at 36.1 and 61.3 θ. The presence of oxycarbide in the CM-n-TiO_2 indicates that doped carbon atoms occupy some oxygen sites in the lattice.

X-ray photoelectron spectroscopy (XPS) survey spectrum (Fig. 5A) of carbon-doped TiO_2, indicated that the sample contains only Ti, O, and C with binding energies for Ti 2p3/2, O 1s, and C 1s are 458.4, 529.7 and 284.8 eV,

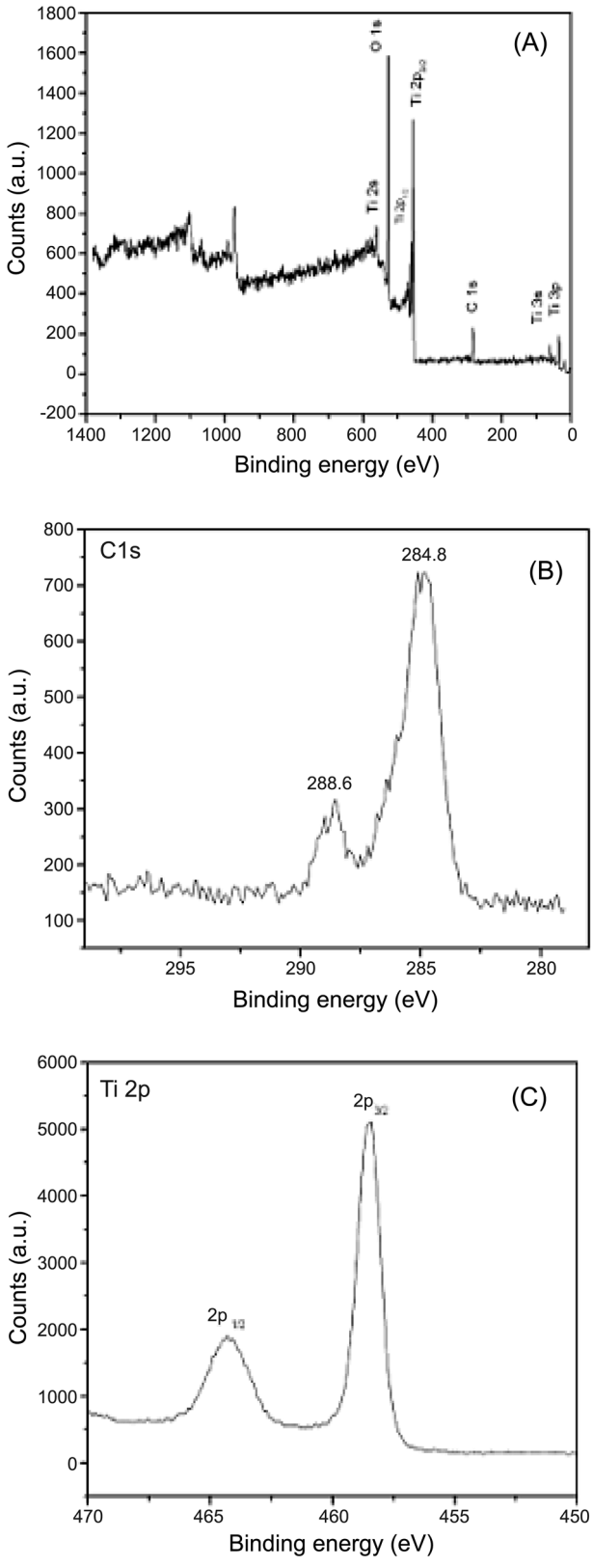

Fig. 5. XPS spectra of (A) survey spectrum, (B) C 1s and (C) Ti 2p for carbon doped titania. (Source: Ref 83).

respectively. The carbon state in the photocatalyst was assessed by C 1s core levels, as shown in Fig. 5B [83]. Two peak structures at the binding energies of 284.8, 288.6 eV were observed for the carbon-doped TiO_2. The peak (284.8 eV) is thought to signal the presence of adventitious elemental carbon and the peak (288.6 eV) indicates the presence of C-O bonds. These data reveal that carbon may substitute for some of the lattice titanium atoms and form a Ti-O-C structure. XPS signals of Ti 2p were observed at binding energies at around 458.5 eV (Ti 2p3/2) and 464.3 eV (Ti 2p1/2), as shown in Fig. 5C. The Ti 2p peaks were in good agreement with pure TiO_2. XPS measurements for C doped TiO_2 material showed a peak due to the Ti-C (281.9 eV).

2.2.3. Visible light application studies

As summarized in Table 1, various dyes namely methylene blue (MB), methyl orange (MO), rhodamine B (RhB) and chlorinated organics such as p-chloro phenol, dioxin, trichloroaectic acid have been tested for PCO under visible light. Apart from these, air pollutants namely CO, acetaldehyde, NOx also examined for their elimination. Visible light water splitting for hydrogen production also reported. These preliminary investigations results are encouraging.

From mechanistic studies Lettmann *et al.* [64] proposed that oxygen plays a major role in the photodegradation with two major reaction pathways,

1. The carbonaceous species acts as a photosensitizer without participation of the titanium dioxide. After excitation of the photosensitizer S, singlet oxygen is formed by a triplet-triplet energy transfer. Alternatively, an electron can be transferred directly from the excited photosensitizer to triplet oxygen to generate the superoxide radical anion $O_2^{\bullet-}$. Both species, singlet oxygen and $O_2^{\bullet-}$, are capable of degrading organic compounds.

2. The excited photosensitizer injects an electron into the conduction band of titanium dioxide (as shown in the equation below). Subsequently, the electron is transferred to

Table 2. Mixed co-doping with carbon

Sl. No	Elements co-doped in TiO_2	Method of Catalyst preparation	Remarks/observation	Application tested	Ref
1.	C & S	Rutile TiO_2 with thiourea calcination at 400-500°C	Atom incorporation (S-0.1%, C-0.2%), In XPS no nitrogen peak, carbonate peak at 288 eV (C 1s binding energy), absorption edge shifted from 400 to 700 nm due to doping	MB dye and 2-methyl pyridine degradation	Ohno *et al.* 2004 [85]
2.	C, S & Ag	TIP treated with ammonium thiocyanate or thiourea and $AgNO_3$. The product was calcined at 500°C for 2 h in air	Nano sized yellow color product with, EDX results of doped material: C-5.5 at%, S-1.7 at% 7 Ag-1.0 at% and no nitrogen, Ag^+ boosted the amount of carbon from 5.5-7.7% due to formation of silver carbonate (IR peak at 761 cm^{-1}), Shift towards longer wave length with band gap lowering to 2.77 eV, Enhanced photo activity due to silver.	Acetaldehyde degradation	Hamal and Klabunde, 2007 [86]
3.	C & N	Mechanochemical method by ball milling of p-25 titania and 10% hexamethylenetetrazine (HMT)	Two absorption edges at 400 & 540 nm	Nitrogen monoxide oxidation	Komatsu *et al.* 2006 [87]
4.	C & N	TIP hydrolysis and coating on glass plate. Doping in an ionized N_2 followed by heating at 500°C for 2 h	$TiO_{2-x-y}N_xC_y$ has two absorption thresholds in visible range (392 & 521 nm) with band gap of 3.06 & 2.22 eV), XPS 398.7 eV due to C-N bond in the film, IR 1719 cm^{-1} due to carbonate	MO dye degradation	Yang *et al.* 2006 [88]
5.	C& N	TTB,urea & TBAH hydrolysis, evaporation to get xerogel and calcinations at 400-500°C	Carbon doping more pronounced than that of nitrogen, carbon species located at the surface of TiO_2 nano particles (no 281 eV EPS peak), Enhanced absorption in the visible region due to co -doping (C& N) synergistic effect	MB dye degradation	Chen *et al.* 2007 [89]
6.	C& N	Mechanochemical doping method of titania with ammonium carbonate & HMT by mixing in a ball mill followed by calcinations at 400°C for 1 h.	Two absorption edges at 408 & (3.04 eV) and 530-550 nm (2.21-2.234 eV), ncreasing mechnochemical stress causes red shift & band gap narrowing, more co-doping with HMT	Nitrogen monoxide oxidation	Yin *et al.* 2007 [90]
7.	N,C, & S	TIP sol gel hydrolysis ,followed by thiourea reaction to form catalyst film on glass plate	1.65, 0.72 and 1.62 wt% N, C&S elements in TiO_2, enhanced photocatalytic activity of the anions doped catalyst	Dioxin degradation	Chu *et al.* 2005 [91]

oxygen adsorbed on the semi-conductor surface producing $O_2^{\bullet-}$.

$$S \xrightarrow{h\nu} S^* \xrightarrow{TiO_2} TiO_2^{\bullet-} + S^+ \xrightarrow{O_2} S^+ + TiO_2 + O_2^{\bullet-}$$

For both pathways to become catalytic, the oxidized photosensitizer has to be reduced again, e.g. by oxidations of organic compounds.

Three reasons may account for the high visible-light activity of C-doped TiO_2. First, C-doped TiO_2 with high surface area can provide more active sites and adsorb more reactive species, which could have been the reason for its enhanced photocatalytic activity. Second, it is considered that the carbon may substitute for some of the lattice titanium atoms close to/on the surface of TiO_2 because the TiO_2 were already formed before doping. Therefore, the band gap narrowing was occurred in the C-doped TiO_2, which could absorb more visible light. These substitutions of surface lattice titanium atoms may explain why doped TiO_2 catalysts with different doping amount of carbon showed similar photocatalytic activities, because surface lattice titanium atoms of the TiO_2 sample had a certain amount, resulting in a limited accommodation for carbon substitutions. Kamisaka *et al.* suggested that cation-doped carbon atoms (carbon at a titanium site) formed a carbonate-type structure by theoretical calculation [58]. This is similar to another carbon-doped TiO_2 photocatalyst reported by Sakthivel and Kisch [60]. Finally, the reduction of organic chemical employed in the hydrothermal process lead to carbonaceous species embedded in the TiO_2 matrix. This may lead to the formation of new active sites, which are also responsible for the observed higher photocatalytic activity.

2.3. Other elements co-doping with carbon

Table 2 presents the studies carried out co-doping of other elements along with carbon. In addition to the above mentioned preparation methods listed in Table 1, mechanochemical method also reported for preparing co-doped catalysts. These materials also characterized using appropriate analytical technique to ascertain the nature of dopant and tested for visible light utility and reported to be efficient. These kinds of co-doped Titania with carbon catalyst materials are likely to play a major role possibly due to their combined effect.

3. Future Trends

From the foregoing it is clear that CDT material has shown promising results for visible light activation. This second generation photocatalyst is a fast developing area and is going to find plenty of applications. Further research and development are necessary in this exciting area. Some indications have been given of the likely areas where current and future research may prove to be of great value in environmental protection. These are

- Fabrication of nm sized c-doped material for maximum activity.
- Investigation on the source of carbon (precursor) employed and method of preparation.
- Improved methods to incorporate most suitable carbon content for solar light use in environmental remediation (PCO) and water splitting to produce hydrogen.
- Simultaneous doping of other materials with carbon in promoting photocatalytic activity.
- Long term stability of TiO_2 C-doped photocatalysts examination.
- Factors improving the solar light photocatalytic activity in general with increased quantum yield.
- Applications such as atmosphere cleaning, wastewater purification, soil remediation and solar cell.
- Pilot scale testing
- More detailed research to understand the visible light activity of CDT.
- Preparation of other C-doped metal oxides (like Zn, Sn, W, Fe, etc.) to modify their properties to find useful applications.

It is hoped that the C-doped titania material with long term stability and low band gap will soon find solar light driven technology for industrial use.

Acknowledgement

Authors are thankful to BK 21-E^2M program for financial support.

References

[1] Fujishima, A.; Honda, K. *Nature* **1972**, *238*, 37.
[2] Diebold, U. *Surface science reports* **2003**, *48*, 53.
[3] Mills, A.; Davies, R. H.; Worsley, D. *Chem. Soc. Rev.* **1993**, *22*, 417.
[4] Fox, M. A.; Dulay, M. T. *Chem. Rev.* **1993**, *93*, 341.
[5] Legrini, O.; Oliveros, E.; Braun, A. M. *Chem. Rev.* **1993**, *93*, 671.
[6] Hoffmann, M. R.; Martin, S. T.; Choi, W.; Bahnemann, D. W. *Chem. Rev.* **1995**, *95*, 69.
[7] Linsebigler, A. L.; Lu, G.; Yates Jr., J. T. *Chem. Rev.* **1995**, *95*, 735.
[8] Hashimoto, K.; Irie, H.; Fujishima, A. *Jap. Jr. App. Phy.* **2005**, *449120*, 8269.
[9] O'Regan, M. Grätzel, *Nature* **1991**, *353*, 737.
[10] Gratzel, M. *Chem. Ing. Tech.* **1995**, *67*, 1300.
[11] Stipkala, J. M.; Castellano, F. N.; Heimer, T. A.; Kelly, C. A.; Livi, K. J. T.; Meyer, G. *J. Chem. Mater.* **1997**, *9*, 2431.
[12] Liska, P.; Vlachopoulos, N.; Nazuddin, M. K.; Comte, P.;

Gratzel, M. *J. Am. Chem. Soc.* **1998**, *110*, 3686.
[13] Peter, L. M.; Wijayantha, K. G. N.; Riely, D. J.; Waggett, J. P. *J. Phys. Chem.* **2003**, *107b*, 8378.
[14] Borgarello, E.; Kiwi, J.; Gratzel, M.; Pelizzetti, E.; Visca, M. *J. Am. Chem. Soc.* **1982**, *104*, 2996.
[15] Iwasaki, M.; Hara, M.; Kawada, H.; Tada, H.; Ito, S. *J. Colloid Interface Sci.* **2000**, *224*, 202.
[16] Klosek, S.; Raftery, D. *J. Phys. Chem. B* **2001**, *105*, 2815.
[17] Zhu, J.; Chen, F.; Zhang, J.; Chen, H.; Anpo, M. *J. Photochem. Photobiol. A* **2006**, *180*, 196.
[18] Yamashita, H.; Ichihashi, Y.; Takeuchi, M.; Kishiguchi, S.; Anpo, M. *J. Synchrotron Rad.* **1999**, *6*, 451.
[19] Herrmann, M.; Disdier, J.; Pichat, P. *Chem. Phys. Lett.* **1984**, *108*, 618.
[20] Karakitsou, K. E.; Verykios, X. E. *J. Phys. Chem.* **1993**, *97*, 1184.
[21] He, C. H.; Gong, J. *Ploy. Deg. & Stability* **2003**, *81*, 117.
[22] Choi, W.; Termin, A.; Hoffmann, M. R. *J. Phys. Chem. B* **1994**, *98*, 13669.
[23] Asahi, R.; Morikawa, T.; Ohwaki, T.; Aoki, K.; Taga, Y. *Science* **2001**, *293*, 269.
[24] Irie, H.; Watanabe, Y.; Hashimoto, K. *Chem. Lett.* **2003**, *32*, 772.
[25] Torres, G. R.; Lindgren, T.; Lu, J.; Granqvist, C. G.; Lindquist, S. E. *J. Phys. Chem. B* **2004**, *108*, 5995.
[26] Lindgren, T.; Mwabora, J. M.; Avendano, E.; Jonsson, J.; Hoel, A.; Granqvist, C. G.; Lindquist, S. E. *J. Phys. Chem. B* **2003**, *107*, 5709.
[27] Burda, C.; Lou, Y. B.; Chen, X. B.; Samia, A. C. S.; Stout, J.; Gole, J. L. *Nano Lett.* **2003**, *3*, 1049.
[28] Morikawa, T.; Asahi, R.; Ohwaki, T.; Aoki, K.; Taga, Y. *Jpn. J. Appl. Phys.* **2001**, *2*, 561.
[29] Sakthivel, S.; Janczarek, M.; Kisch, H. *J. Phys. Chem. B* **2004**, *108*, 19384.
[30] Irie, H.; Watanabe, Y.; Hashimoto, K. *J. Phys. Chem. B* **2003**, *107*, 5483.
[31] Nakamura, R.; Tanaka, T.; Nakato, Y. *J. Phys. Chem. B* **2004**, *108*, 10617.
[32] Prokes, S. M.; Gole, J. L.; Chen, X.; Burda, C.; Carlos, W. E. *Adv. Funct. Mater.* **2005**, *15*, 161.
[33] Li, D.; Haneda, H.; Hishita, S.; Ohashi, N. *Mat. Sci. Eng. B* **2005**, *117*, 67.
[34] Sathis, M.; Viswanathan, B.; Viswanath, R. P. *Appl. Cat. B Env.* **2007**, *74*, 308.
[35] Umebayashi, T.; Yamaki, T.; Itoh, H.; Asai, K. *Appl. Phys. Lett.* **2002**, *81*, 454.
[36] Ohno, T.; Mitsui, T.; Matsumura, M. *Chem. Lett.* **2003**, *32*, 364.
[37] Ohno, T.; Akiyoshi, M.; Umebayashi, T.; Asai, K.; Mitsui, T.; Matsumura, M. *Appl. Catal. A Gen.* **2004**, *265*, 115.
[38] Tachikawa, T.; Tojo, S.; Kawai, K.; Endo, M.; Fujitsuka, M.; Ohno, T.; Nishijima, K.; Miyamoto, Z.; Majima, T. *J. Phys. Chem. B* **2004**, *108*, 19299.
[39] Pore, V.; Ritala, M.; leskcla, M.; Areva, S.; Jarn, M.; Jarnstrom, J. *J. Mat. Chem.* **2007**, *17*, 1361.
[40] Yamaki, T.; Umebayashi, T.; Sumita, T.; Yamamoto, S.; Maekawa, M.; Kawasuso, A.; Itoh, H. *Nuc. Inst. Meth. Phy. Res. B* **2003**, *206*, 254.
[41] Li, D.; Haneda, H.; Hishita, S.; Ohashi, N.; Labhsetwar, N. K. *J. Fluorin. Chem.* **2005**, *126*, 69.
[42] Li, D.; Haneda, H.; Labhsetwar, N. K.; Hishita, S.; Ohash, N. *Chem. Phy. Let.* **2005**, *401*, 579.
[43] Huang, D. G.; Liao, S. J.; Dang, Z.; Petrik, L. *J. Photo-Chem. Photobio.* **2006**, *184*, 282.
[44] Kim, H.; Choi, W. *Appl. Cat. B Env.* **2007**, *69*, 127.
[45] Araña, J.; Doña-Rodríguez, J. M.; Tello Rendón, E.; González-Díaz, C.; Herrera-Melián, J. A.; Pérez-Peña, J.; Colón, G.; Navío, J. A. *Appl. Catal. B Environ.* **2003**, *44*, 161.
[46] Matos, J.; Laine, J.; Herrmann, J. M. *J. Catal.* **2001**, *200*, 10.
[47] Tryba, B.; Morawski, A. W.; Inagaki, M. *Appl. Catal. (B) Env.* **2003**, *46*, 203.
[48] Tryba, B.; Morawski, A. W.; Inagaki, M. *Appl. Cata. (B) Env.* **2003**, *41*, 427.
[49] Inakagi, M.; Kjin, F.; Tryba, B.; Toyoda, M. *Carbon* **2005**, *43*, 1652.
[50] Janus, M.; Tryba, B.; Inagaki, M.; Morawski, A. W. *Appl. Cata. (B) Env.* **2004**, *52*, 61.
[51] Lin, L.; Zhou, Y.; Xhu, Y.; Xie, Y. *Front. Chem. China* **2007**, *2*, 64.
[52] Chen, M. L.; Ko, Y. S.; Oh, W. C. *Carbon Science* **2007**, *8*(1), 6.
[53] Kwon, O. H.; Jang, J. S.; Palanivelu, K.; Lee, Y. S. *The Carbon Society Conference Proceedings*, Gwang ju **2007**, 23.
[54] Su, B.; Liu, X.; Peng, X.; Xiao, T.; Su, Z. *Mat. Sci. Eng.* **2003**, *A349*, 59.
[55] Makarova, O. V.; Rajh, T.; Thurnauer, M. C. *Env. Sci. Tech.* **2000**, *34*, 4797.
[56] Fung, A. K. M.; Chiu, B. K. W.; Lam, M. H. W. *Wat. Res.* **2003**, *37*, 1939.
[57] Cronemeyer, D. C. *Phys. Rev.* **1959**, *113*, 1222.
[58] Kamisaka, H.; Adachi, T.; Yamashita, K. *J. Chem. Phy.* **2005**, *123*, 084704.
[59] Valentin, C. D.; Pacchioni, G.; Selloni, A. *Chem. Mater.* **2005**, *17*, 6656.
[60] Sakthivel, S.; Kisch, H. *Angew. Chem. Int. Ed.* **2003**, *42*, 4908.
[61] Li, Y.; Hwang, D. S.; Lee, N. H.; Kim, S. J. *J. Chem. Phys. Lett.* **2005**, *404*, 25.
[62] Lee, J. Y.; Park, J.; Cho, J. H. *Appl. Phy. Let.* **2005**, *87*, 011904.
[63] Xu, T. H.; Song, C. I.; Liu, Y.; Han, G. R. *J. Zhejiang Univ. Science B* **2006**, *7*, 299.
[64] Lettmann, C.; Hildenbrand, K.; Kisch, H.; Macyk, W.; Maier, W. F. *Appl. Catal. B Env.* **2001**, *32*, 215.
[65] Khan, S. U. M.; Al-Shahry, M.; Ingler Jr. W. B. *Science*

2002, *297*, 2243.
[66] Choi, Y.; Umebayashi, T.; Yamamoto, S.; Tanaha, S. *J. Mat. Sci. Let.* **2003**, *22*, 1209.
[67] Choi, Y.; Umebayashi, T.; Yoshikawa, M. *J. Mater. Sci.* **2004**, *39*, 1837.
[68] Ohno, T.; Tsubota, T.; Nishijima, K.; Miyamoto, Z. *Chem. Lett.* **2004**, *33*, 750.
[69] Martyana, I. N.; Uma, S.; Rodrigues, S.; Klabunde, K. *J. Chem. Comm.* **2004**, *24*, 2476.
[70] Shankar, K.; Paulose, M.; Mor, G. K.; Varghese, O. K.; Grimes, C. A. *J. Phys. D Appli. Phy.* **2005**, *38*, 3543.
[71] Neummann, B.; Bogdanoff, P.; Tributsch, H.; Sakthivel, S.; Kisch, H. *J. Phys. Chem. B* **2005**, *109*, 16579.
[72] Reddy, K. M.; Baruwati, B.; Jayalakshmi, M.; Rao, M. M.; Manorama, S. V. *J. Solid State Chemistry* **2005**, *178*, 3352.
[73] Tseng, Y. H.; Kuo, C. S.; Huang, C. H.; Li, Y. Y.; Chou, P. W.; Cheng C. L.; Wong, M. S. *Nanotechnology* **2006**, *17*, 2490.
[74] Chou, P. W.; Treschev, S.; Chung, P. H.; Cheng, C. L.; Tseng, Y. H.; Chen, Y. J.; Wong, M. S. *Appl. Phys. Lett.* **2006**, *89*, 131919.
[75] Shen, M.; Wu, Z.; Huang, H.; Du, Y.; Zou, Z.; Yang, P. *Materials Letters* **2006**, *60*, 693.
[76] Irie, H.; Washizuka, S.; Hashimoto, K. *Thin Solid Films* **2006**, *510*, 21.
[77] Xu, C.; Killmeyer, R.; Gray, M. L.; Khan, S. U. M. *Electrochemistry Communication* **2006**, *8*, 1650.
[78] Park, J. H.; Kim, S. W.; Bard, A. *J. Nano. Lett.* **2006**, *6*, 24.
[79] Enache, C. S.; Schoonman, J.; van de Krol, R. *Appl. Surface Sci.* **2006**, *252*, 6342.
[80] Barnes, P. R. F.; Randeniya, L. K.; Murphy, A. B.; Gwan, P. B.; Plumb, I. C.; Glasscock, J. A.; Grey, I. E.; Li, C. *Dev. Chem. Eng. Miner. Process.* **2006**, *14*, 51.
[81] Xu, C.; Shaban, Y. A.; Ingler Jr., W. B.; Khan, S. U. M. *Solar Energy Materials & Solar Cells* **2007**, *91*, 938.
[82] Xu, C.; Khan, S. U. M. *Electrochem.Solid.St.* **2007**, *10*, B56.
[83] Ren, W.; Ai, Z.; Jia, F.; Zhang, L.; Fan, X.; Zou, Z. *Appl. Catal. B Env.* **2007**, *69*, 138.
[84] Hahn, R.; Ghicov, A.; Salonen, J.; Lehto, V. P.; Schmuki, P. *Nanotechnology* **2007**, *18*, 105604.
[85] Ohno, T.; Tsubota, T.; Toyofuku, M.; Inaba. R. *Catal. Lett.* **2004**, *98*, 255.
[86] Hamal, D. B.; Klabunde, K. J. *J. Colloid and Interface Science* **2007**, *311*, 514.
[87] Shu, Y.; Komatsu, M.; Qiwu, Z.; Ruixing, L.; Qing, T.; Saito, F.; Sato, T. *The Chinese Journal of Process Engineering* **2006**, *6*, 478.
[88] Yang, J.; Bai, H.; Tan, X.; Lian, *J. Applied Surface Science* **2006**, *253*, 1988.
[89] Chen, D.; Jiang, Z.; Geng, J.; Wang, Q.; Yang, D. *Ind. Eng. Chem. Res.* **2007**, *46*, 2741.
[90] Yin, S.; Komatsu, M.; Zhang, Q.; Saito, F.; Sato, T. *Mater. Sci.* **2007**, *42*, 2399.
[91] Chu, S. Z.; Inoue, S.; Wada, K.; Li, D.; Suzuki, J. *Langmuir* **2005**, *21*, 8035.